ISSN: 2457-0400

Impact Factor: 7.675

WORLD JOURNAL OF ADVANCE HEALTHCARE RESEARCH

www.wjahr.com

Volume: 10, Issue: 7

Page N. 358-364

Year: 2026

Original Article

Coden USA: WJAMA3

SYNTHESIS, DYEING PERFORMANCE, AND CORROSION INHIBITION OF A NOVEL RESORCINOL-BASED MANNICH BASE

Malak Alhori*, Abdulilah Alsheikh Hammoud

[1]Department of Chemistry, Homs University, Homs, Syria.

Article Received: 05 June 2026 **Article Revised: 25 June 2026** **Article Published: 03 July 2026**

***Corresponding Author: Malak Alhori**

Department of Chemistry, Homs University, Homs, Syria.

DOI: https://doi.org/10.5281/zenodo.21155693

How to cite this Article: Malak Alhori*, Abdulilah Alsheikh Hammoud (2026). Synthesis, Dyeing Performance, And Corrosion Inhibition Of A Novel Resorcinol-Based Mannich Base. World Journal of Advance Healthcare Research, 10(7), 358–364.

ABSTRACT

In this study, a novel resorcinol derivative was synthesized via a catalyst-free three-component Mannich reaction between resorcinol and 2,4-dinitrophenylhydrazine. The reaction proceeded successfully, and the product was isolated as a yellow precipitate. The synthesized compound was fully characterized using Fourier transform infrared spectroscopy (FT-IR), as well as ^{1}H NMR and ^{13}C NMR spectroscopy. The FT-IR spectrum confirmed the formation of a new methylene bridge, evidenced by characteristic absorption bands at 2859–2922 cm^{-1}, indicating the success of the Mannich reaction. The ^{1}H NMR and ^{13}C NMR spectra further corroborated the proposed structure, displaying distinctive signals for the methylene bridge at 3.45 ppm and 43 ppm, respectively. The dyeing performance of the synthesized compound was evaluated on wool and cotton fibers, demonstrating good affinity and coloration efficiency, particularly for wool fibers. Furthermore, the compound was assessed as a corrosion inhibitor for carbon steel in 3.5 wt.% NaCl solution using electrochemical polarization techniques. The results revealed excellent inhibition performance, achieving a maximum efficiency of 99.3% at an optimal concentration of 150 ppm.

KEYWORDS: Mannich reaction; Resorcinol derivative; Wool dyeing; Corrosion inhibition; Carbon steel; Electrochemical polarization.

1. INTRODUCTION

Phenols and their derivatives have garnered significant attention from researchers due to their versatile applications across various fields. In the industrial sector, these compounds are primarily utilized in the production of synthetic dyes, tanning processes, and the manufacturing of advanced polymers, including plastics, adhesives, and rubber.[1] Additionally, they serve as crucial additives for gasoline, lubricating oils, and energetic materials.[2] In the biomedical field, the phenolic hydroxyl group holds paramount importance due to its direct role in a wide array of biological activities.[3]

Within this important chemical family, resorcinol (1,3-dihydroxybenzene) stands out as a phenolic compound of particular significance. Most of its derivatives exhibit antioxidant activity[4], and studies have demonstrated cytotoxic activity against cancer cells.[5] Resorcinol has a long history of topical therapeutic use, particularly in the treatment of acne and seborrheic dermatitis, leveraging its keratolytic properties.[6] Accumulating recent data indicate its diverse biological activities, including antimicrobial and antiparasitic properties.[7] Its derivatives, manufactured according to the Mannich reaction, were of great importance.

The Mannich reaction represents a powerful condensation method between active hydrogen compounds, an aldehyde, and an amine (or amine-like derivatives), leading to the formation of multi-functional Mannich bases. Depending on the reaction center, these bases are classified into C-, N-, S-, and P-Mannich bases. Phenolic Mannich bases are categorized under C-Mannich bases due to the formation of a robust C–C bond, representing a highly significant class of compounds owing to their diverse biological and industrial activities.[8]

Although resorcinol-based Mannich bases have been extensively studied, their potential as dual-functional agents combining textile dyeing and corrosion inhibition has received limited attention. This study aims to explore this dual functionality by evaluating the synthesized resorcinol derivative as a dye for natural fibers and as a corrosion inhibitor for carbon steel.

Herein, we report the design and synthesis of a novel resorcinol derivative via a catalyst-free three-component Mannich reaction of resorcinol with 2,4-dinitrophenylhydrazine. The synthesized compound was fully characterized and evaluated for its dual-functional capabilities: as a dye for natural fibers and as an efficient corrosion inhibitor for carbon steel in a 3.5 wt.% NaCl medium.

2. MATERIAL AND METHODS

2.1. Materials and Instruments: All chemicals and reagents used in this work were of analytical grade, purchased from BDH, Sigma-Aldrich, and Merck, and were used as received without further purification. The Fourier-transform infrared (FT-IR) spectrum was recorded on a JASCO FT/IR-4100 spectrophotometer in the range of (4000–400cm^{-1})using KBr pellets. The ^{1}H and ^{13}C nuclear magnetic resonance (NMR) spectra were recorded on a Bruker 400 M_{HZ} spectrometer using d_6-DMSO as the solvent. Chemical shifts (δ) are reported in parts per million (ppm) relative to tetramethylsilane (TMS) as an internal standard. Electrochemical measurements were performed using a Gill AC potentiostat/galvanostat (ACM Instruments, UK) equipped with a conventional three-electrode corrosion cell.

2.2. Preparation of 4-((2-(2,4-Dinitrophenyl) hydrazinyl)methyl)benzene-1,3-diol via Mannich Reaction.

A mixture of 2,4-dinitrophenylhydrazine (0.396 g, 2.0 mmol) and 37% aqueous formaldehyde (1.0 mL, 13.4 mmol) in acetonitrile (24 mL) was charged into a 100 mL round-bottom flask equipped with a magnetic stirrer and a reflux condenser. The reaction mixture was stirred at 25 °C for 1 h. Subsequently, resorcinol (0.22 g, 2.0 mmol) was added portion-wise, and the stirring was maintained at 82 °C for an additional 7 h. The progress of the reaction was monitored by thin-layer chromatography (TLC) using a mixture of dichloroethane/chloroform (1:1 v/v) as the mobile phase. After the reaction was complete, the mixture was allowed to cool to room temperature. The resulting yellow precipitate was collected by filtration, washed with cold distilled water, and dried. The crude product was then dissolved in hot ethanol. Upon cooling, the unreacted 2,4-dinitrophenylhydrazine precipitated and was removed by filtration. The filtrate was then left to evaporate at room temperature, affording the pure title compound as a yellow solid. Yield: 85%; Melting point. 168–169 °C.

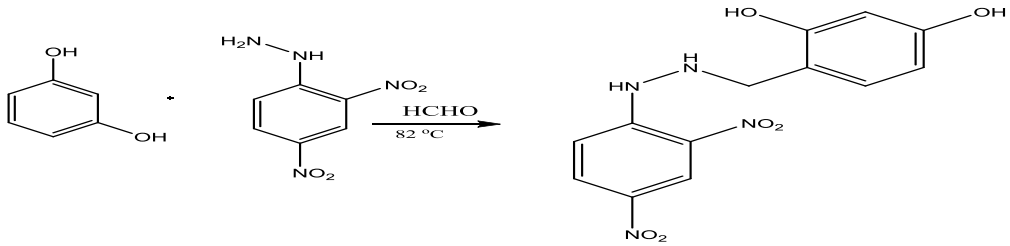

Scheme 1. Synthetic pathway of the novel resorcinol derivative via the Mannich reaction.

Figure 1: Physical appearance and isolated crystal form of the synthesized resorcinol Mannich base.

Figure 2: TLC chromatogram visualized using an iodine vapor chamber, showing the R_f values of the synthesized product (R_f = 0.84), starting resorcinol (R_f = 0.08), and 2,4-dinitrophenylhydrazine (R_f = 0.53).

3. RESULTS AND DISCUSSION

4-((2-(2,4-dinitrophenyl)hydrazineyl)methyl)benzene-1,3-diol compound was characterized using FT-IR ^{1}H-NMR and ^{13}C-NMR.

3.1.The FT-IR spectrum (Fig. 3) confirms the success of the Mannich reaction. The primary evidence is the disappearance of the starting material's primary amine bands, along with the emergence of new bands at 2922–2895 cm^{-1} assigned to the methylene bridge (-CH_2-). The broad absorption between 3463–3557 cm^{-1} is due to the phenolic stretching vibrations. Furthermore, the bands of the hydrazine moiety appear at 3414 and 3304 cm^{-1}. The aromatic system is indicated by the stretching at 3089 cm^{-1} and the skeletal vibrations in the 1510–1614 cm^{-1} region. The nitro groups (-NO_2) showed their typical symmetric and asymmetric stretching. Figure 4 and Table 1 illustrate the difference between the infrared spectra of the raw materials and the product.

3.2. NMR characterization

3.2.1. The 1H NMR spectrum (Fig. 5) (400 MHz, DMSO-d_6) shows a distinctive singlet signal at 3.451 ppm (s, 2H), which is unambiguously assigned to the methylene bridge (-CH2-), confirming the success of the Mannich reaction. The phenolic protons (-OH) appear as a broad singlet at 11.478 ppm (br s, 2H). The hydrazine moiety exhibits two distinct singlet signals at 9.054 ppm (s, 1H) and 4.354 ppm (s, 1H), corresponding to the respective nitrogen-bound protons (-NH-). In the aromatic region, the protons of the resorcinol and dinitrophenyl rings appear as a series of multiple and double signals in the range of 6.601–8.839 ppm, which is perfectly consistent with the expected substitution pattern.

3.2.2.The ^{13}C NMR spectrum (Fig. 6) (100 MHz, DMSO-d_6) further substantiates the structural framework, displaying the characteristic methylene carbon signal at 43.069 ppm. The aromatic carbons of both rings are resolved as a series of sharp signals at 111.216, 120.538, 123.344, 129.922, 130.413, 137.750, 138.878, 141.620, 145.182, 153.642, 155.808, and 154.632 ppm.

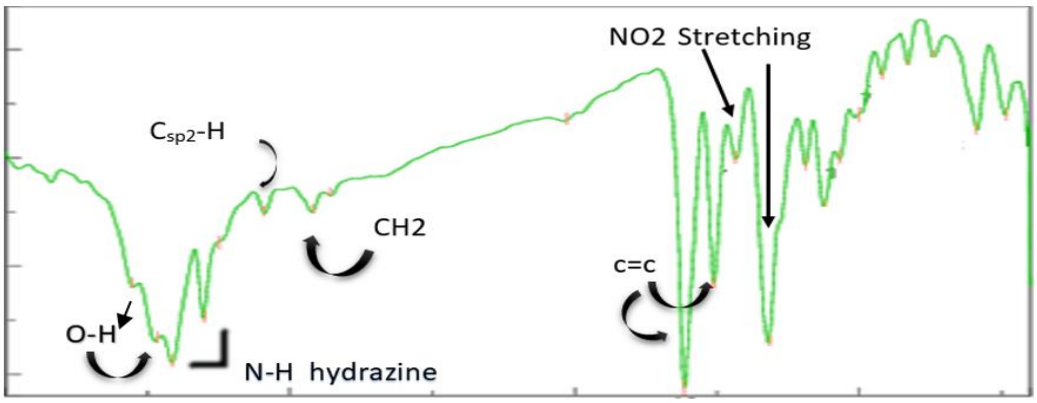

Fig. 3: FT-IR spectrum of 4-((2-(2,4-dinitrophenyl)hydrazinyl)methyl)benzene-1,3-diol.

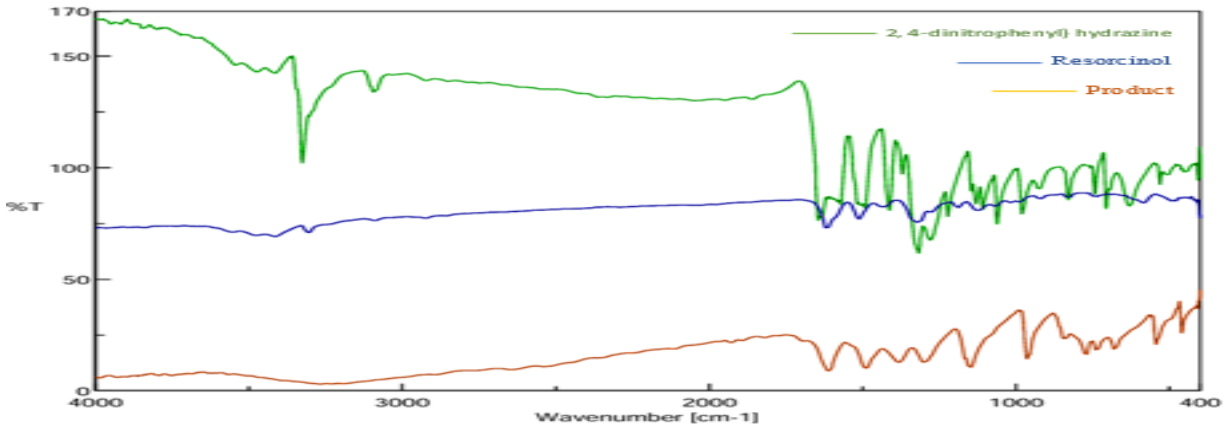

Fig. 4: Comparative FT-IR spectra of the reactants and the final synthesized compound.

Table 1: Characteristic IR absorption bands cm^{-1} of the starting materials and the synthesized product.

Comp.	C_{SP3}-H2(ῡ)	-NH2 (ῡ)	-NH (ῡ)	-OH (ῡ)
The product	Asym 2922 cm^{-1} sym 2859 cm^{-1}	-	3463-3557 cm^{-1}	3304.43-3414.35 cm^{-1}
Resorcinol	-	-	-	3231.15-3266.82 cm^{-1}
2,4-dinitrophenylhydrazine	-	Asym 3463 cm^{-1} Sym 3418 cm^{-1}	3326.61 cm^{-1}	-

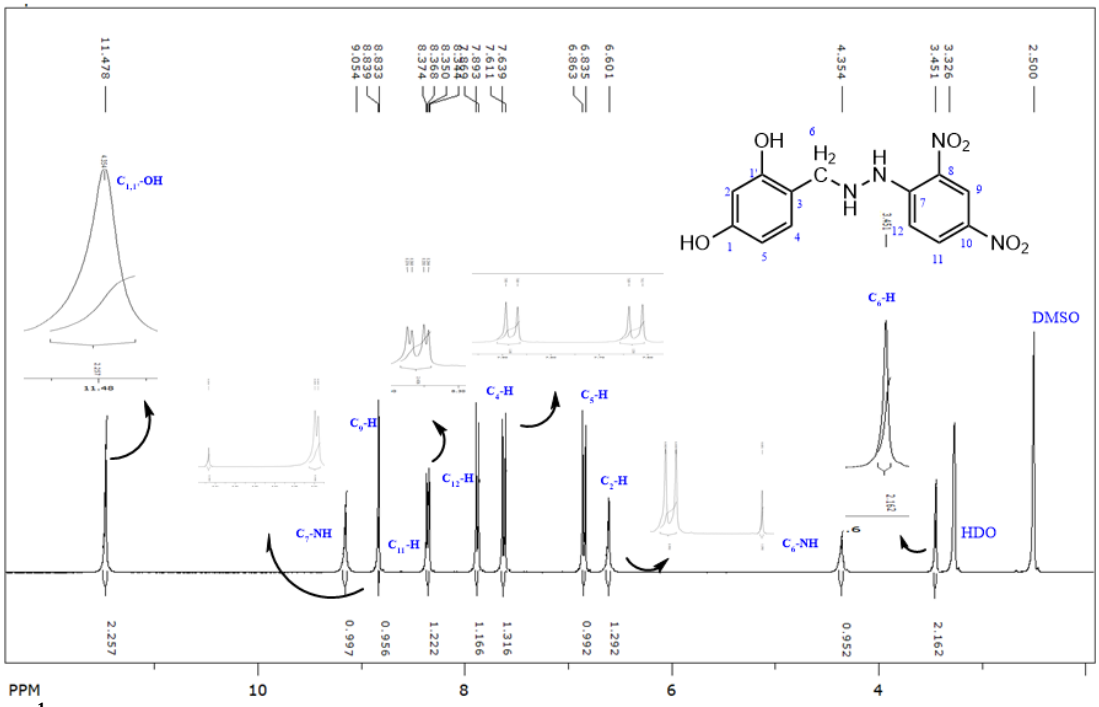

Fig.5. ^{1}H-NMR Spectroscopic Analysis of 4-((2-(2,4-dinitrophenyl)hydrazinyl)methyl)benzene-1,3-diol.

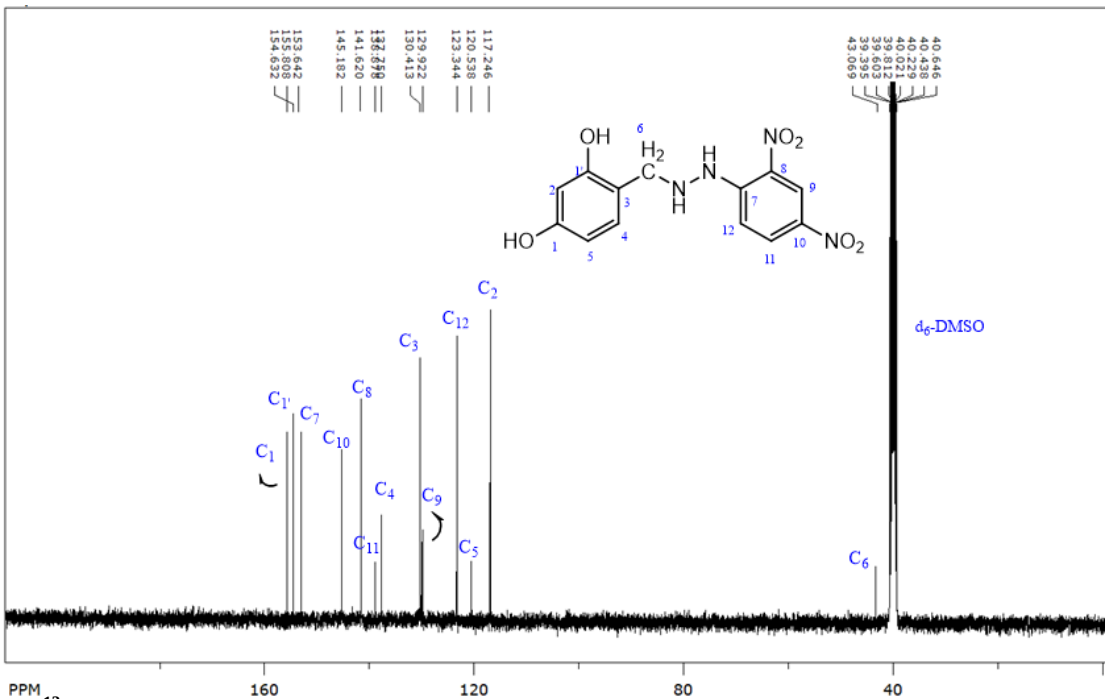

Fig.6. ^{13}C-NMR Spectroscopic Analysis of 4-((2-(2,4-dinitrophenyl)hydrazinyl)methyl)benzene-1,3-diol.

4. Dyeing Performance and Coloration Potential on Natural Fibers

To explore the functional versatility and coloration potential of the newly synthesized Mannich base, a preliminary dyeing study was comprehensively conducted on natural cellulose (cotton) and protein (wool) fibers. The dyeing process was performed at 60 °C for 90 min under controlled pH environments optimized for each fiber type (pH 9 for cotton and pH 4 for wool). As illustrated in Figure 12, both fabrics exhibited a significant and uniform color transformation from white to distinct, stable shades. Specifically, the cotton fabric displayed a light orange hue, whereas the wool fiber acquired a distinct brown coloration. This successful fixation is inherently driven by the multifunctional architecture of the synthesized derivative, which contains rich hydrogen-bonding and electrostatic donor/acceptor sites (such as hydroxyl, nitro, and hydrazine moieties) capable of interacting efficiently with the polymeric matrices of the fibers.

Under the alkaline conditions (pH 9), the hydroxyl groups of the cotton cellulose undergo partial deprotonation, facilitating intermolecular hydrogen bonding and dipole-dipole interactions with the nitro and phenolic groups of the synthesized dye, locking the molecular framework within the cellulose structure. Conversely, under acidic conditions (pH 4), the amino groups within the protonated protein chains of the wool fibers experience strong electrostatic attractions with the electron-dense regions of the synthesized Mannich base, resulting in the observed deep brown coloration.[9]

Fig.12: Visual appearance of cotton and wool fabrics before (left) and after (right) the dyeing process with the synthesized Mannich base derivative. The distinct shades of orange and reddish-brown confirm the successful fixation and chemical affinity of the dye under the specified pH conditions (pH 9 for cotton and pH 4 for wool).

5. Electrochemical Corrosion Inhibition and Adsorption Isotherm

The corrosion inhibition efficiency of the synthesized compound was evaluated on a carbon steel working electrode in 3.5 wt. % NaCl solution at a controlled temperature of 25 °C. Prior to each electrochemical measurement, the working electrode surface was mechanically polished with a series of silicon carbide (SiC) emery papers (from 400 to 2000 grit). It was then rinsed with distilled water, degreased with acetone, and dried with a hot air stream. Electrochemical measurements were conducted using a three-electrode corrosion cell connected to a Gill AC potentiostat/galvanostat (ACM Instruments, UK). Different concentrations of the inhibitor (ranging from 75 to 300 ppm) were prepared by dissolving them in a minimum volume of dimethyl sulfoxide (DMSO) prior to addition to the saline solution. A stainless steel rod was used as the counter electrode, and an Ag/AgCl (saturated KCl) electrode was employed as the reference electrode. Prior to performing the polarization measurements, the open circuit potential (OCP) was recorded for 60 min until a stable potential was achieved. Finally, the inhibition efficiency (η%) and surface coverage degree (θ) were calculated based on the corrosion current density (I_corr) values extrapolated from the Tafel plots.[10] Electrochemical Tafel Polarization Measurements Based on the Reduction of Corrosion Current Density.

$$\eta\% = \left(\frac{Iblank - Icorr}{Iblank}\right) \times 100$$

and surface coverage degree

$$\theta = \frac{\eta\%}{100} = \left(\frac{Iblank - Icorr}{Iblank}\right)$$

and were compared with the values recorded for the aqueous medium containing the same amount of DMSO and salt (blank).

As shown in Table 3, the corrosion current density (I_corr) decreased sharply from 291 µA cm^{-2} in the blank solution to 2.02 µA cm^{-2} upon the addition of 150 ppm of the inhibitor. This noticeable decrease was accompanied by an increase in the inhibition efficiency, reaching a maximum value of 99.31% at this concentration. The corrosion potential (E_corr) shifted significantly from −650.98 mV (blank) to −77.68 mV at 150 ppm, corresponding to a positive shift of approximately +573 mV. This substantial displacement towards more positive potentials indicates that the synthesized compound acts predominantly as an anodic-type inhibitor, primarily retarding the anodic dissolution of iron through the formation of a protective adsorbed layer on the metal surface. The significant reduction in corrosion current density, combined with the large positive shift in E_corr, confirms the strong anodic inhibition mechanism of the synthesized Mannich base.

Table 3: Electrochemical polarization parameters for carbon steel corrosion in 3.5 wt.% NaCl solution in the absence and presence of various concentrations of the synthesized Mannich base inhibitor.

Concentration (ppm)	Corrosion Current Density (I_{corr} uA/cm^2)	Corrosion Potential (E_{corr} ,mv)	Surface Coverage(Ɵ)	Inhibition Efficiency (%)
0	291.00	-650.98	0.000	0.00%
75	18.40	-77.75	0.937	93.68%
150	2.02	-77.68	0.993	99.31%
300	9.35	-87.77	0.968	96.79%

Table 4: **Thermodynamic parameters derived from the Langmuir adsorption isotherm for the synthesized inhibitor on carbon steel surface in 3.5 wt.% NaCl solution at 298.15 K.**

Adsorption Type	ΔG°_{ads} (kJ/mol)	K_{ads}(L/mol)	Correlation Coefficient (R^2)	Linear Regression Equation
Chemisorption	-44.95	1.384×10^6	0.9998	y = 1.0287x + 0.243

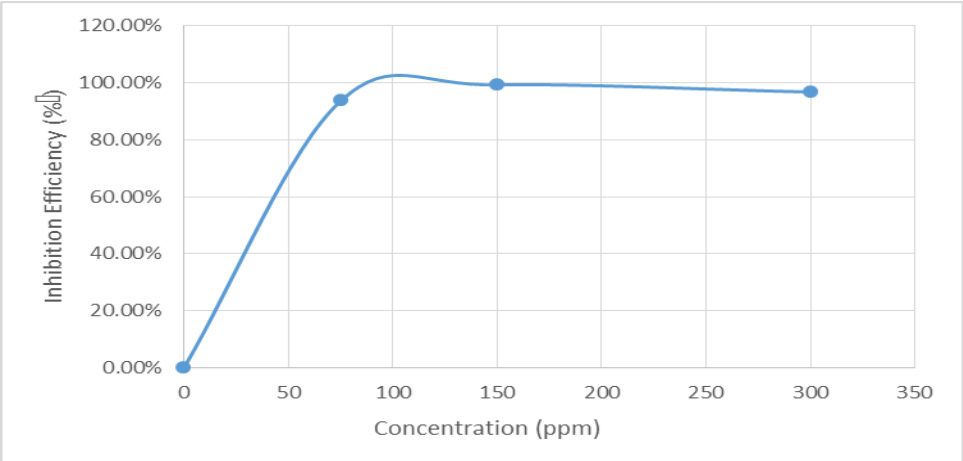

Figure 4: ***Variation of inhibition efficiency (η%) as a function of inhibitor concentration for carbon steel in 3.5 wt.% NaCl solution at 298.15 K.***

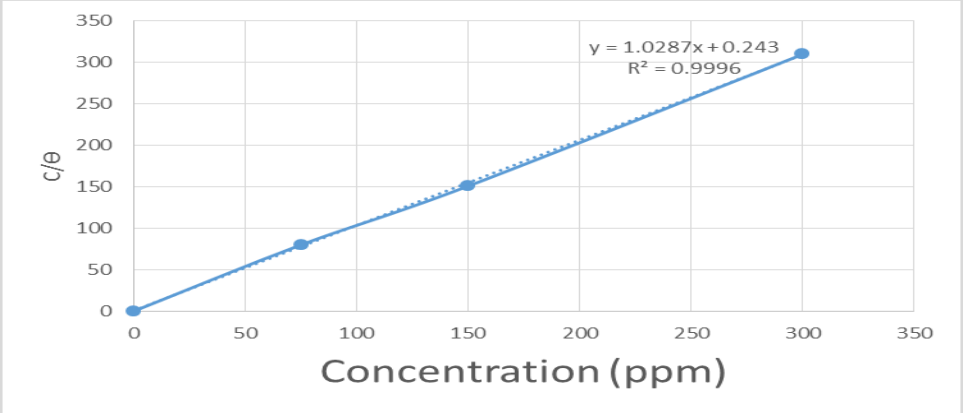

Figure 5: ***Langmuir adsorption isotherm plot for the synthesized Mannich base on carbon steel surface in 3.5 wt.% NaCl solution at 298.15 K.***

Interestingly, when the inhibitor concentration was increased beyond the optimal dose (from 150 ppm) to (300ppm), a slight decrease in the inhibition efficiency (%) from (99.31%) to (96.79%) was observed. This behavior is mainly attributed to the molecular aggregation or partial micellization of the dissolved molecules at high concentrations, which significantly reduces the number of free molecules (monomers) available for adsorption on the active iron sites. Furthermore, steric hindrance and electrostatic repulsion between the closely packed organic molecules at a concentration of (300 ppm) may induce partial desorption or a change in the optimal spatial orientation for surface adsorption, thereby causing a slight re-exposure of the active sites to the corrosive medium.[10]

6. CONCLUSION

In conclusion, a novel resorcinol derivative was successfully synthesized via an environmentally friendly, catalyst-free three-component Mannich reaction using resorcinol and 2,4-dinitrophenylhydrazine. The chemical structure of the synthesized Mannich base was firmly confirmed through comprehensive FT-IR, ^{1}H NMR, and ^{13}C NMR spectroscopic analyses. The synthesized compound demonstrated good dyeing affinity toward wool fibers, exhibiting effective coloration under the applied conditions. Most prominently, electrochemical investigations established that this compound acts as an efficient corrosion inhibitor for carbon steel in 3.5 wt.% NaCl solution, achieving an exceptional protection efficiency of 99.3% at an optimal concentration of 150 ppm. The elimination of catalyst requirements, combined with its promising performance in both textile dyeing and corrosion inhibition, highlights the economic and sustainable value of this newly synthesized compound.

ACKNOWLEDGMENTS

The authors would like to express their sincere gratitude to the Faculty of Science and the Faculty of Chemical Engineering at Homs University for providing the necessary facilities, administrative support, and environment to conduct this research.

REFERENCES

1. Gaitan E. Environmental goitrogenesis. CRC Press, 1989 Mar 31.
2. Albuquerque BR, Heleno SA, Oliveira MB, Barros L, Ferreira IC. Phenolic compounds: Current industrial applications, limitations and future challenges. Food & function, 2021; 12(1): 14-29.
3. Tahir T, Ashfaq M, Saleem M, Rafiq M, Shahzad MI, Kotwica-Mojzych K, Mojzych M. Pyridine scaffolds, phenols and derivatives of azo moiety: current therapeutic perspectives. Molecules, 2021 Aug 11; 26(16): 4872.
4. Otsubo M, Sakimoto K, Egami H, Hamashima Y. Dearomative enantio-and diastereoselective difluorination of resorcinol derivatives. Tetrahedron, 2021 Sep 10; 96: 132355.
5. Zheng Y, Wu FE. Resorcinol derivatives from Ardisia maculosa. Journal of Asian natural products research, 2007 Sep 1; 9(6): 545-9.
6. Romagnoli C, Baldisserotto A, Vicentini CB, Mares D, Andreotti E, Vertuani S, Manfredini S. Antidermatophytic action of resorcinol derivatives: ultrastructural evidence of the activity of phenylethyl resorcinol against Microsporum gypseum. Molecules, 2016 Sep 30; 21(10): 1306.
7. Stasiuk M, Kozubek A. Biological activity of phenolic lipids. Cellular and Molecular life sciences, 2010 Mar; 67(6): 841-60.
8. Tokalı FS, Taslimi P, Demircioğlu İH, Şendil K, Tuzun B, Gülçin İ. Novel phenolic Mannich base derivatives: synthesis, bioactivity, molecular docking, and ADME-Tox Studies. Journal of the Iranian Chemical Society, 2022 Feb; 19(2): 563-77.
9. Broadbent AD. Basic principles of textile coloration, society of dyers and colourists. West Yorkshire, UK, 2001.
10. Kokalj A. On the use of the Langmuir and other adsorption isotherms in corrosion inhibition. Corrosion Science, 2023 Jun 1; 217: 111112.